

# $d_{x^2-y^2}$ Pairing of Composite Excitations in the 2D Hubbard Model

Tudor D. Stanescu, Ivar Martin\*, and Philip Phillips

*Loomis Laboratory of Physics  
University of Illinois at Urbana-Champaign  
1100 W.Green St., Urbana, IL, 61801-3080*

We report on a strong coupling approach (on-site Coulomb repulsion,  $U$  larger than the nearest-neighbour hopping energy  $|t|$ ) to the Hubbard model. Starting from the Hubbard operators which diagonalize the interaction term, we generate a hierarchy of composite operators from the equations of motion. Using the Hubbard operators as a basis, we are able to compute the associated Green functions including the anomalous Green functions which describe pair formation. We show explicitly that these anomalous Green functions are non-zero in the  $d_{x^2-y^2}$  channel; however, the entities that pair up are not single electron-like particles but rather composite excitations (which we call cexons) made out of an electron and a hole on nearest-neighbour sites. Cexons are fermionic in nature as they have spin 1/2 and also have unit charge. Our calculations of the chemical potential reveal that negative compressibility in the 2D Hubbard model and composite excitation pairing are intimately connected, namely, the larger the negative compressibility, the larger the pairing amplitude. Our observation of negative compressibility in the under-doped regime is consistent with phase segregation or stripe formation in the normal state. While pairing ameliorates the negative compressibility, it does not eliminate it entirely. In addition, we find that the anomalous correlation functions are particle-hole symmetric and exhibit a maximum at a doping level of roughly 10% as measured from half-filling. For  $U = 8|t|$ , the onset temperature for pair formation is  $0.02|t|$ . The effect of nearest-neighbour Coulomb repulsions is discussed.

## I. INTRODUCTION

After a protracted quest [1] for superconductivity in the Hubbard model, it is surprising that the question is still open. This state of affairs has arisen primarily because the parameter space in which superconductivity is anticipated to reside is precisely the strong coupling limit,  $U \gg |t|$ , in which traditional perturbative schemes fail. As a result, progress on this question has relied predominantly on exact diagonalization or Quantum Monte Carlo (QMC) simulations on finite systems. While early work [1] showed promising results on the possible onset of superconducting pair correlations in the 2D Hubbard model, the most recent numerical work [2] shows that true superconductivity with at least algebraic decay of anomalous correlations is absent. In light of such results, it has also been suggested that some combination of phonons [3] and or next nearest-neighbour hopping [4] are needed for superconductivity to survive. Further, Kuroki and Aoki [5] have suggested that QMC simulations have yet to access the energy scale of order  $0.01t$  where strong-coupling superconductivity [6] is expected to occur. In addition, Beenen and Edwards [7] have analyzed the 2D Hubbard model with an equations of motion technique considerably enhanced by Mancini, Matsumoto, and co-workers [8] and shown that pairs with  $d_{x^2-y^2}$  symmetry emerge. However, this work has key weaknesses: the onset temperature and the window of doping over which  $d_{x^2-y^2}$  pairing occurs are highly sensitive to the decoupling scheme of the anomalous Green functions. For ex-

ample, at least order of magnitude variations in the onset temperature were observed [7] for  $U = 8|t|$  and a decoupling scheme which is supposedly exact in the limit of  $U \rightarrow \infty$  resulted in a near vanishing of pairing for  $U > 10|t|$ .

Despite these difficulties, the Hubbard model remains central to such strongly correlated problems as superconductivity in the cuprates as well as the organic conductors. In fact, in so far as the motion of holes in the  $\text{CuO}_2$  planes in the cuprates can be modeled realistically [9] by the Hubbard model in the vicinity of half-filling, the microscopic underpinnings of the pairing mechanism in these materials should arise from this model. Because  $D=2$  is the marginal dimension for superconductivity, it might be that while the pairing mechanism originates within a single layer, interlayer tunneling is needed to maintain long-range phase coherence. Hence, the questions that face the Hubbard model are three-fold: 1) does local pairing of the right sort obtain to describe the cuprates, 2) what entities are involved in the pairing, and 3) is long-range phase coherence present? In this work we develop a strong-coupling approach that is sufficient to answer the first two questions. Our approach is based on a simple observation first made by Hubbard [10]. Namely, that the bare electron annihilation operator can be written as a sum of two composite operators

$$c_{i\sigma} = c_{i\sigma}n_{i-\sigma} + c_{i\sigma}(1 - n_{i-\sigma}) = \eta_{i\sigma} + \xi_{i\sigma}. \quad (1)$$

The quantities described by  $\eta_{i\sigma}$  and  $\xi_{i\sigma}$  are composite excitations. The  $\eta$  excitation describes an electron restricted to move on sites already occupied with an elec-

tron of opposite spin whereas  $\xi$  demands that there be no prior occupancy on the site. A key feature these operators possess is that they exactly solve the  $t = 0$  Hubbard model. Consequently, an equation of motion approach based on these operators will lead naturally to an expansion in  $t/U$ . Such an expansion is ideally suited for the strong coupling regime  $U \gg |t|$  in which both the cuprates as well as the organic conductors reside. It is this approach that we pursue here.

When the kinetic energy is treated as a perturbation, hybridization is introduced into the Hubbard atomic orbital basis. As a result,  $\xi_i$  and  $\eta_i$  are no longer the eigenoperators. The new type of excitations can be thought of heuristically as resonant valence-bond hybrids. To determine what operators create such excitations, it is sufficient to construct the equations of motion for the Hubbard operators. The relevant operators have the kinetic energy,  $t$  as a coefficient. As we will see, the simplest terms that arise are of the form,  $\eta_{ij\sigma} = c_{i\sigma}n_{j\tau}$  with  $(ij)$  nearest neighbours. This operator is the generator of a composite excitation (or cexon) that is restricted to live on sites  $i$  with a nearest neighbour site  $j$  occupied. Such composites have unit charge as can be seen directly from the commutator,

$$[\eta_{ij\sigma}, n_{l\sigma'}] = \delta_{\sigma,\sigma'} \delta_{il} \eta_{ij\sigma}. \quad (2)$$

Also, quite obviously, its spin is  $1/2$ . In fact, all the composite excitations generated in our scheme have unit charge. Hence, spin and charge are coupled. However, while the  $\eta_{ij}$  excitation is fermionic in character, it is not confined to a single site. Rather, it is an excitation that lives on neighbouring sites. In traditional perturbative schemes, such as Fermi liquid theory, similar composite operators naturally appear. However, in such approaches, the operators that are generated do not describe new excitations but rather dress the non-interacting quasiparticles. In this approach, the new operators do in fact describe fundamentally new excitations [11] as they give rise to new peaks in the spectral function. The appearance of new peaks in the spectral function is incompatible with a Fermi liquid description of the composite excitations.

It might be argued that the emergence of cexons in this model and the unrecoverability of Fermi liquid theory are inevitable in an approach based fundamentally on the atomic limit of the Hubbard model. However, any theory of high  $T_c$  must be based on a starting point that captures the essence of strong-correlation physics. While the atomic limit might seem extreme, it is justified in this context as  $U \gg t$  in high  $T_c$  systems. Consequently, it stands to reason that the physically-relevant excitations should bear a greater family resemblance to the atomic limit eigentates than they would to the plane-wave excitations which populate the non-interacting limit. Cexons are the simplest local excitations that arise once the Hubbard operators are hybridized on nearest-neighbour sites.

To determine if such excitations really do constitute new particles in the strongly-coupled limit, dynamical corrections must be included to the theory we present below.

As in earlier composite operator approaches [7,8,12,13], we find that the traditional correlation function,  $\langle c_{i\uparrow}c_{j\downarrow} \rangle$ , does *not* determine the pairing gap in the 2D Hubbard model. Rather

$$\theta_{ij} = \langle c_{i\uparrow}c_{i\downarrow}n_{j\tau} \rangle = \langle \eta_{ij\uparrow}\eta_{ij\downarrow} \rangle \quad (3)$$

is the relevant anomalous correlation function that determines pairing in the d-wave channel. The emergence of this correlation function as the d-wave order parameter in the Hubbard model and the seemingly innocuous rewriting (overlooked previously in similar Green function analyses [7,8]) in terms of the  $\eta_{ij\sigma}$  operators is particularly illuminating. Pairing based on the  $\eta_{ij\sigma}$  excitations is the new feature which we develop explicitly in this work. This rewriting signifies that composite excitations rather than electron-like particles, as would be the case in a traditional Fermi liquid, are involved in the pairing process in a strongly-correlated system with repulsive interactions. In addition, the fact that the new composite operators describe the pairing lends further credence to their correspondence with new excitations in the strongly-correlated regime. While it is well known that quasiparticles in strongly-correlated systems do not resemble well electron-like excitations, as shown, for example, by the absence of a sharp peak at the Fermi surface in angle-resolved photoemission experiments [14] on the under-doped normal state of the cuprates, the traditional mechanism invoked to explain this fact is spin-charge separation [9,15]. In 1-dimension [16] spin-charge separation is on firm footing. In addition, even in a singlet BCS superconductor, spin-charge separation occurs naturally as the Cooper pairs carry charge but no spin, whereas the quasiparticles are spin  $1/2$  but have no well-defined charge. In  $D=2$ , fractionalization of the electron also occurs in the fractional quantum Hall effect [17,18]. For strongly-correlated systems, spin-charge separation has been proposed based on a slave-boson picture [19–27]. However, recently Nayak [28] has shown that the slave particles always remain confined. Our work suggests that rather than falling apart, electrons form clusters or composites when the Coulomb interaction is large and repulsive. Such entities form pairs in the 2D Hubbard model. We propose that composite excitations of the kind we describe here offer a natural explanation for the absence of electron-like excitations in the ARPES experiments [14] on the underdoped cuprates. While it is tempting to draw a connection between pairing of composite excitations in the 2D Hubbard model and the pairing of composite fermions [29] in quantum Hall systems, this connection would be tenuous at best.

Our approach then accomplishes two things: 1) First we are able to access the strong-coupling limit of the

Hubbard model and identify the relevant composite excitations. 2) We are able to show that such composites pair in the  $d_{x^2-y^2}$  channel. Our work then represents a formulation of d-wave pairing from a microscopic model out of which emerges a hierarchy of new composite fermionic excitations. We find that the magnitude of the anomalous correlation function for composite excitation pairing increases as the compressibility in the normal state becomes more negative. In the next section, we outline the essential details of the strong-coupling approach. In Sec. III, we derive the equations of motion for the composite excitations and all the relevant correlation functions. The results for the anomalous pairing correlation functions are presented in Sec. IV.

## II. FORMALISM

The starting point of our analysis is the on-site Hubbard model

$$H = - \sum_{i,j,\sigma} t_{ij} c_{i\sigma}^\dagger c_{\sigma j} + U \sum_i n_{i\uparrow} n_{i\downarrow} - \mu \sum_i n_i \quad (4)$$

where  $t_{ij} = t$  if  $(i, j)$  are nearest-neighbour sites and zero otherwise,  $\mu$  is the chemical potential and  $U$  the on-site Coulomb repulsion. Consider the retarded Green function

$$\langle\langle c_{i\uparrow}; c_{j\downarrow} \rangle\rangle = \theta(t - t') \langle\{c_{i\uparrow}(t), c_{j\downarrow}(t')\}\rangle \quad (5)$$

where  $\{A, B\}$  is the anticommutator. As a result of the interaction term in Eq. (4), the equation of motion for this Green function will generate a new Green function that is proportional to  $\langle\langle [c_{i\uparrow}, H]; c_{j\downarrow} \rangle\rangle$ . This Green function will contain the composite excitation  $\eta_{i\sigma}$ . All higher-order Green functions will emerge from time derivatives of composite operators. This suggests that we should start with the Hubbard operators,  $\eta_{\sigma i} = c_{i\sigma} n_{i-\sigma}$  and  $\xi_{\sigma}(i) = c_{i\sigma}(1 - n_{i-\sigma})$  introduced previously. The utility of these operators is immediate. Their commutator with the interaction part of the Hubbard model yields  $-(\mu - U)\eta_{i\sigma}$  and  $-\mu\xi_{i\sigma}$ , respectively. Hence, they can be used to diagonalise the  $t = 0$  Hubbard model. Consequently, if this basis is used to compute correlation functions, all higher-order correlation functions that will be generated will be multiplied by the hopping term. That is, these operators form the basis for a  $t/U \ll 1$  or equivalently a strong coupling expansion. The essence of this approach was first proposed by Linderberg and Öhrn [30] and has been applied to the Hubbard model [7,31,32] as well as the p-d model for the cuprates [33].

To illustrate the utility of the composite operator technique, we switch to the 4-component basis,

$$\psi(i) = \begin{pmatrix} \xi_{i\uparrow} \\ \eta_{i\uparrow} \\ \xi_{i\downarrow}^\dagger \\ \eta_{i\downarrow}^\dagger \end{pmatrix}. \quad (6)$$

Let us define

$$j(i) = i\partial_t \psi(i) = [\psi(i), H] \quad (7)$$

as the ‘current’ operator. Formally, we can write the  $n^{\text{th}}$  element of the current as

$$j_n(i) = \sum_m K_{nm} \psi_m(i) + \delta j_n(i). \quad (8)$$

We can project out the part of the correction,  $\delta j$ , that is ‘orthogonal’ to the composite operator basis by rewriting

$$\delta j_n = \sum_{ml} \langle\{\delta j_n, \psi_m^\dagger\}\rangle I_{ml}^{-1} \psi_l + \delta \phi_n, \quad (9)$$

where  $\delta \phi$  satisfies the equation,  $\{\delta \phi, \Psi^\dagger\} = 0$ . Let us introduce the normalization matrix

$$I_{il} = \langle\{\psi_i, \psi_l^\dagger\}\rangle = \frac{\Omega}{(2\pi)^2} \int d^2 k e^{i\mathbf{k}\cdot(\mathbf{r}_i - \mathbf{r}_l)} I(\mathbf{k}) \quad (10)$$

and the overlap matrix

$$M_{il} = \langle\{j_i, \psi_l^\dagger\}\rangle = \frac{\Omega}{(2\pi)^2} \int d^2 k e^{i\mathbf{k}\cdot(\mathbf{r}_i - \mathbf{r}_l)} M_{il}(\mathbf{k}) \quad (11)$$

where  $\mathbf{k}$ -integration is over the Brillouin zone and  $\Omega$  the inverse area of the Brillouin zone. The elements of the  $\mathbf{I}$  and  $\mathbf{M}$  matrices contain only the mutual correlations among the constituents of the composite operator basis. Because  $\{\delta \phi, \Psi^\dagger\} = 0$ , we can write the overlap matrix as

$$\mathbf{M} = \mathbf{E}\mathbf{I} \quad (12)$$

where

$$E_{nm} = K_{nm} + \sum_l \langle\{\delta j_n, \psi_l^\dagger\}\rangle I_{lm}^{-1}. \quad (13)$$

This matrix (the energy matrix) will play a crucial role in our approach. Because of the  $\delta j$  contribution, the energy matrix contains higher order correlations which are not expressible as simple correlations of the  $\psi$ -fields. It is from the  $\delta j$  terms that the composite excitations arise. Consequently, the higher-order correlation functions must either be decoupled or used as self-consistent parameters in equations obtained by imposing various symmetries, such as the Pauli principle [8,32]. As a result of the orthogonality of  $\delta \phi$  to the composite operator basis, we will neglect the contribution from  $\delta \phi$  in all subsequent calculations. This approximation is equivalent to ignoring the dynamical corrections to the self-energy. Such contributions are expected to be small because the

Hubbard operator basis solves exactly the  $U = \infty$  limit. The principal role of  $\delta\phi$  is to broaden the energy levels associated with the composite operator spectrum. The role of such dynamical corrections will be the focus of future study. Within this approximation, we can write any Green function

$$S(i, j) = \langle\langle \psi(i); \psi^\dagger(j) \rangle\rangle \quad (14)$$

in Fourier space as

$$S(\mathbf{k}, \omega) = (\omega - \mathbf{E}(\mathbf{k}))^{-1} \mathbf{I}(\mathbf{k}) \quad (15)$$

by using the equations of motion. This equation and the expression,  $\mathbf{M} = \mathbf{E}\mathbf{I}$ , are the central equations of this approach. The  $\mathbf{M}$  and  $\mathbf{I}$  matrices involve correlation functions which can be obtained self-consistently and by introducing symmetry properties such as the Pauli principle [32] to close the equations of motion. It is the off-diagonal blocks of the energy matrix that contain information about anomalous pairing correlations.

There are three types of self-consistent equations that enter this approach. The simplest of these involves the correlations between the  $\psi$  fields that appear in  $\mathbf{M}$  and  $\mathbf{I}$ . The general expression for such correlation functions in terms of the corresponding Green function is given by

$$\begin{aligned} \langle \psi_m(i) \psi_n^\dagger(j) \rangle &= \frac{\Omega}{(2\pi)^2} \int d^2k d\omega e^{i\mathbf{k}\cdot(\mathbf{r}_i - \mathbf{r}_j)} (1 - f(\omega)) \\ &\times \left( \frac{-1}{\pi} \right) \text{Im} S_{mn}(\mathbf{k}, \omega) \\ &\equiv C_{m,n}(i, j) \end{aligned} \quad (16)$$

with  $f(\omega)$  the Fermi-Dirac distribution function. The self-consistency of Eq. (16) follows from the dependence of  $\mathbf{E}$  and  $\mathbf{I}$  on correlations in the composite operator basis. To obtain explicitly the self-consistent equations, we rewrite Eq. (15) as

$$S(\mathbf{k}, \omega) = \sum_{i=1,2} \left[ \frac{\kappa_i^+}{\omega - \epsilon_i + i\eta} + \frac{\kappa_i^-}{\omega + \epsilon_i - i\eta} \right] \quad (17)$$

where

$$\kappa_i^\pm = \frac{\lambda(\pm\epsilon_i)}{\pm 2\epsilon_i(\epsilon_i^2 - \epsilon_j^2)} \quad (18)$$

with  $(i, j)$  chosen from  $(1, 2)$  but  $i \neq j$ ,  $\epsilon_i$  the eigenvalues of the energy matrix and the matrix  $\lambda$  is given by

$$\lambda(\omega) = \text{Det}(\omega\mathbf{1} - \mathbf{E})(\omega\mathbf{1} - \mathbf{E})^{-1} \mathbf{I}. \quad (19)$$

The four eigenvalues correspond to the four composite operator bands:  $i=1,2$  refer to the  $\xi$  and  $\eta$  bands, respectively, whereas  $+$ ,  $-$  index the particle and hole states, respectively. If we now use Eq. (17) in Eq.(16), we obtain the general self-consistent equation,

$$C_{m,n}(i, l) = \frac{\Omega}{2(2\pi)^2} \int d^2k e^{i\mathbf{k}\cdot(\mathbf{r}_i - \mathbf{r}_l)} \left[ I_{mn} + \sum_{i=1,2} ((\kappa_i^+)_{mn} - (\kappa_i^-)_{mn}) \right] \tanh \frac{\beta\epsilon_i}{2} \quad (20)$$

for correlation functions within the composite operator basis where  $T = 1/k_B\beta$ .

It is well-known that in approximation schemes of this sort, certain correlation functions which vanish explicitly as a result of the Pauli principle, self-consistently iterate to a non-zero value. To avoid this shortcoming, we explicitly maintained the symmetries [8,32] imposed by the Pauli principle, namely

$$C_{1,2}(i, i) = \langle \xi_\sigma(i) \eta_\sigma^\dagger(i) \rangle = 0. \quad (21)$$

This is the second type of self-consistent integral equation that will be used in this method. Likewise,  $C_{2,1}(i, i) = 0$ . As a result of imposing these symmetry relations, we will find that our theory is completely particle-hole symmetric about half-filling.

The final self-consistent equations arise from decoupling correlations of composite fields that are not contained in the basis described by Eq. (6). This procedure will be described in detail in the next section.

### III. COMPUTATIONAL MACHINERY

#### A. Equations of Motion

We start first by constructing the algebra

$$\{\xi_i, \xi_j^\dagger\} = \delta_{ij} \left( \mathbf{1} + \frac{1}{2} \sigma^\mu n_\mu \right) \quad (22)$$

$$\{\eta_i, \eta_j^\dagger\} = -\delta_{ij} \frac{1}{2} \sigma^\mu n_\mu \quad (23)$$

$$\{\xi_i, \xi_j\} = \{\eta_i, \eta_j\} = \{\xi_i, \eta_j^\dagger\} = 0 \quad (24)$$

of the composite operators, with  $\sigma^\mu$  for  $\mu = 1, 2, 3$  are the Pauli matrices,  $\sigma^0$  is the identity matrix, and

$$-\frac{1}{2} \sigma^\mu n_\mu = \begin{pmatrix} n_{i\downarrow} & -c_{i\downarrow}^\dagger c_{i\uparrow} \\ -c_{i\uparrow}^\dagger c_{i\downarrow} & n_{i\uparrow} \end{pmatrix}. \quad (25)$$

From these equations, it follows that the I-matrix is given by

$$I = \begin{pmatrix} 1 - \frac{n}{2} & 0 & 0 & \Delta_0 \\ 0 & \frac{n}{2} & -\Delta_0 & 0 \\ 0 & -\Delta_0^* & 1 - \frac{n}{2} & 0 \\ \Delta_0^* & 0 & 0 & \frac{n}{2} \end{pmatrix} \quad (26)$$

where  $\Delta_0 = \langle c_{i\uparrow} c_{i\downarrow} \rangle$  and we have assumed that  $\langle n_\uparrow \rangle = \langle n_\downarrow \rangle = n/2$ . We now turn to the ‘‘current’’. We can construct the ‘‘current’’ from the equations of motion

$$j(i) = i \frac{\partial}{\partial t} \psi(i) = [\psi(i), H] \quad (27)$$

for the  $\psi$ -fields with

$$j_1(i) = -\mu \xi_{i\uparrow} - \sum_j t_{ij} c_{j\uparrow} - 4t\pi_{i\uparrow} \quad (28)$$

$$j_2(i) = -(\mu - U)\eta_{i\uparrow} + 4t\pi_{i\uparrow} \quad (29)$$

$$j_3(i) = \mu \xi_{i\downarrow}^\dagger + \sum_j t_{ij} c_{j\downarrow}^\dagger + 4t\pi_{i\downarrow}^\dagger \quad (30)$$

$$j_4(i) = (\mu - U)\eta_{i\downarrow}^\dagger - 4t\pi_{i\downarrow}^\dagger \quad (31)$$

and

$$4t \begin{pmatrix} \pi_{i\uparrow} \\ \pi_{i\downarrow} \end{pmatrix} = \sum_j t_{ij} \begin{pmatrix} -n_{i\downarrow} c_{j\uparrow} + c_{i\downarrow}^\dagger c_{i\uparrow} c_{j\downarrow} - c_{i\uparrow} c_{i\downarrow} c_{j\downarrow}^\dagger \\ -n_{i\uparrow} c_{j\downarrow} + c_{i\uparrow}^\dagger c_{i\downarrow} c_{j\uparrow} + c_{i\uparrow} c_{i\downarrow} c_{j\uparrow}^\dagger \end{pmatrix}.$$

We also need the M-matrix. The distinct elements of this matrix are

$$\begin{aligned} M_{11}(\mathbf{k}) &= FT\langle\{j_1, \xi_\uparrow^\dagger\}\rangle = -\mu(1 - \frac{n}{2}) - 4te \\ &\quad - 4t\alpha(\mathbf{k})(1 - n + p) \\ M_{12}(\mathbf{k}) &= FT\langle\{j_1, \eta_\uparrow^\dagger\}\rangle = 4te - 4t\alpha(\mathbf{k})(\frac{n}{2} - p) \\ M_{22}(\mathbf{k}) &= FT\langle\{j_2, \eta_\uparrow^\dagger\}\rangle = -(\mu - U)\frac{n}{2} - 4te - 4tap \\ M_{13}(\mathbf{k}) &= FT\langle\{j_1, \xi_\downarrow\}\rangle = -4t\gamma(\mathbf{k})\theta + 8t\alpha\Delta_0 - 4t\Delta_{c\xi} \quad (32) \\ M_{14}(\mathbf{k}) &= FT\langle\{j_1, \eta_\downarrow\}\rangle = -(\mu + 4t\alpha(\mathbf{k}))\Delta_0 \\ &\quad + 4t\gamma(\mathbf{k})\theta - 4t\Delta_{c\eta} \\ M_{23}(\mathbf{k}) &= FT\langle\{j_2, \xi_\downarrow\}\rangle = (\mu - U - 4t\alpha(\mathbf{k}))\Delta_0 \\ &\quad + 4t\gamma(\mathbf{k})\theta + 4t\Delta_{c\xi} \\ M_{24}(\mathbf{k}) &= FT\langle\{j_2, \eta_\downarrow\}\rangle = -4t\gamma(\mathbf{k})\theta + 4t\Delta_{c\eta} \end{aligned}$$

with the normal correlations

$$e = \langle \xi_i^\alpha \xi_i^\dagger \rangle - \langle \eta_i^\alpha \eta_i^\dagger \rangle, \quad (33)$$

and

$$p = \langle n_{i\sigma} n_{i\sigma}^\alpha \rangle + \langle c_{i\uparrow}^\dagger c_{i\downarrow} (c_{i\downarrow}^\dagger c_{i\uparrow})^\alpha \rangle - \langle c_{i\uparrow} c_{i\downarrow} (c_{i\downarrow}^\dagger c_{i\uparrow}^\dagger)^\alpha \rangle, \quad (34)$$

and anomalous correlations

$$\Delta_{c\xi} = \langle c_{i\uparrow} \xi_{i\downarrow}^\alpha \rangle - \langle c_{i\downarrow} \xi_{i\uparrow}^\alpha \rangle, \quad (35)$$

$$\Delta_{c\eta} = \langle c_{i\uparrow} \eta_{i\downarrow}^\alpha \rangle - \langle c_{i\downarrow} \eta_{i\uparrow}^\alpha \rangle, \quad (36)$$

and

$$\theta = \langle c_{i\uparrow} c_{i\downarrow} [n_\uparrow(\mathbf{r}_i + \hat{x}) + n_\downarrow(\mathbf{r}_i + \hat{x})] \rangle. \quad (37)$$

In these equations,  $FT$  signifies the Fourier transform as defined in Eq. (11),  $\alpha$  represents an average over nearest-neighbour sites,  $\hat{x}$  indexes nearest-neighbour sites, and  $\alpha(\mathbf{k}) = \cos k_x + \cos k_y$ . Unlike  $\alpha(\mathbf{k})$  which is the coefficient of the normal correlation functions, the Fourier

coefficient  $\gamma(\mathbf{k})$  is a coefficient of an anomalous correlation function. Hence, it is sensitive to the sign change of the anomalous correlation functions as  $\exp(i\mathbf{k} \cdot \mathbf{r})$  is summed over nearest neighbour sites. For s-wave symmetry,  $\alpha(\mathbf{k}) = \gamma(\mathbf{k})$  while for d-wave symmetry  $\gamma(\mathbf{k}) = \cos k_x - \cos k_y$ . The symmetry relationships among the elements of  $\mathbf{M}$  are as follows:

$$\begin{aligned} M_{11} &= -M_{33} \\ M_{12} &= -M_{34} \\ M_{22} &= -M_{44} \\ M_{14} &= -M_{32}^*. \end{aligned} \quad (38)$$

The  $M_{13}$ ,  $M_{14}$ ,  $M_{23}$ , and  $M_{24}$  contain the anomalous correlation functions in particular the  $\theta$  correlation discussed in the introduction.

With the  $\mathbf{M}$  and  $\mathbf{I}$ -matrices in hand, we now construct the energy matrix. From the structure of the normalization matrix and the symmetry properties of the  $\mathbf{M}$  matrix (Eq. (38)), it follows that the energy matrix is of the form,

$$\mathbf{E} = \begin{pmatrix} \mathbf{A} & \mathbf{B} \\ \mathbf{B} & -\mathbf{A} \end{pmatrix}, \quad (39)$$

where  $\mathbf{A}$  and  $\mathbf{B}$  are  $2 \times 2$  matrices. The off-diagonal blocks of the energy matrix determine the gap in the energy spectrum induced by pairing. To isolate the relevant parts of the normalization and  $\mathbf{M}$  matrices that enter the energy gap, we consider the candidate pairing symmetries. No simplifications occur in the s-channel. However, we have verified that none of the anomalous correlation functions are non-zero either in this channel. The same state of affairs occurs in p-wave symmetry. What about d-wave symmetry? Here several significant simplifications occur. First, as a result of the nodes in the gap, no purely on-site anomalous correlation functions survive. As a consequence,  $\langle c_{i\uparrow} c_{i\downarrow} \rangle = \Delta_0 = 0$ . This leads to a vanishing of all the off-diagonal blocks of the normalization matrix. Consequently, only the off-diagonal blocks of the  $\mathbf{M}$ -matrix enter the off-diagonal elements of the energy matrix. However, further simplifications occur. Consider for example,  $\Delta_{c\xi}$  and  $\Delta_{c\eta}$  in Eqs. (35) and (36). These quantities are symmetrized and in addition involve a sum over the nearest neighbour sites in the Brillouin zone. Consequently, they vanish identically in the d-wave channel. The only anomalous correlation function that remains is  $\theta$ , Eq. (37). At this level of theory, this is the only correlation function that does not vanish by symmetry conditions. This is the only anomalous correlation function that enters the gap in the energy spectrum. Hence, as advertised, any pairing will necessarily be governed by a non-traditional correlation function. This correlation function involves a composite operator that lives on a cluster of nearest-neighbour sites. By defining  $\eta_{ij\sigma}$  to be  $c_{i\sigma} n_{j\tau}$ , we rewrite Eq. (37) as Eq.

(3) in which it is clear that pairing in  $\theta$  occurs between two composite excitations.

## B. Computational Procedure

What remains to be done is the calculation of the anomalous correlation functions. Our assumption of singlet pairing implies that

$$\langle c_{i\uparrow}c_{i\downarrow}n_{j\tau} \rangle = \langle c_{i\uparrow}c_{i\downarrow}n_{j-\tau} \rangle = \langle c_{i\downarrow}^\dagger c_{i\uparrow}^\dagger n_{j\tau} \rangle^*. \quad (40)$$

Consequently, we can define  $\theta$  as

$$\theta = 2\langle c_{i\uparrow}c_{i\downarrow}n_{j\tau} \rangle \quad (41)$$

where the spin  $\tau$  is arbitrary. As this correlation function involves more than two basis operators, it must be decoupled. We will follow a procedure analogous to that devised by Roth [31] in her treatment of the strong-coupling limit of the Hubbard model. To implement the Roth method, we consider the Green function

$$H(i, j, t, t') = \langle \langle c_{i\downarrow}^\dagger(i, t); c_{i\uparrow}(j, t')^\dagger n_\sigma(j, t') \rangle \rangle. \quad (42)$$

Clearly, if this Green function is calculated,  $\theta$  can be obtained directly from an expression analogous to Eq. (16). We proceed by constructing the series of Green functions,

$$\begin{aligned} A_\sigma(i, j, k, t, t') &= \langle \langle \xi_\uparrow(i, t); c_\uparrow(j, t')^\dagger n_\sigma(k, t') \rangle \rangle \\ B_\sigma(i, j, k, t, t') &= \langle \langle \eta_\uparrow(i, t); c_\uparrow(j, t')^\dagger n_\sigma(k, t') \rangle \rangle \\ F_\sigma(i, j, k, t, t') &= \langle \langle \xi_\downarrow^\dagger(i, t); c_\uparrow(j, t')^\dagger n_\sigma(k, t') \rangle \rangle \\ G_\sigma(i, j, k, t, t') &= \langle \langle \eta_\downarrow^\dagger(i, t); c_\uparrow(j, t')^\dagger n_\sigma(k, t') \rangle \rangle \end{aligned} \quad (43)$$

in which the creation operator at time  $t$  is replaced by each of the composite operators in the 4-component basis. The Green function of interest,  $H$ , is obtained by summing  $F$  and  $G$  and setting  $i = j$ . To calculate these quantities, we use the equations of motion for  $\psi$ , Eq. (7), and in particular the approximation that  $j = i\partial_t\psi \approx E\psi$ . Consequently, the equations of motion for the Green functions,

$$i\partial_t \begin{pmatrix} A_\sigma \\ B_\sigma \\ F_\sigma \\ G_\sigma \end{pmatrix} = E(i) \begin{pmatrix} A_\sigma \\ B_\sigma \\ F_\sigma \\ G_\sigma \end{pmatrix} + i\delta(t-t') \begin{pmatrix} f_{1\sigma} \\ f_{2\sigma} \\ f_{3\sigma} \\ f_{4\sigma} \end{pmatrix} \quad (44)$$

are directly related to the energy matrix in real space,  $E(i)$  and the term,  $f_{n\sigma} = \langle \langle \psi_n(i, t), c_\uparrow(j, t)^\dagger n_\sigma(k, t) \rangle \rangle$ , that arises from the equal-time anticommutation of  $\psi$  with the composite operators in the Green function. Note that in general,  $f_n$  is a linear combination of correlation functions in the composite operator basis and correlations associated with  $A + B$  or  $F + G$ . Consequently, we

now have a closed set of equations from which  $\theta$  can be obtained.

In the next step, we Fourier transform these equations of motion so that  $t \rightarrow \omega$ ,  $r_k - r_i \rightarrow k_1$ , and  $r_j - r_i \rightarrow k_2$ . Noting that  $\omega - E = IS^{-1}$ , we obtain

$$\begin{pmatrix} A_\sigma(k_1, k_2, \omega) \\ B_\sigma(k_1, k_2, \omega) \\ F_\sigma(k_1, k_2, \omega) \\ G_\sigma(k_1, k_2, \omega) \end{pmatrix} = S(k_1 + k_2, \omega) I^{-1} \begin{pmatrix} f_{1\sigma}(k_1, k_2) \\ f_{2\sigma}(k_1, k_2) \\ f_{3\sigma}(k_1, k_2) \\ f_{4\sigma}(k_1, k_2) \end{pmatrix}$$

To extract  $\theta$  from these equations, we sum  $F$  and  $G$ , integrate over  $k_2$  so that  $i = j$  and then using Eq. (16), we find that

$$\theta = \frac{2\zeta}{\phi + 1} \quad (45)$$

where

$$\phi = \frac{n^2 - 4D}{n(2 - n)} \quad (46)$$

$$\begin{aligned} \zeta &= \frac{2}{2 - n} (C_{11}(i, j) + C_{12}(i, j)) (C_{13}(i, j) + C_{14}(i, j)) \\ &\quad + \frac{2}{n} (C_{22}(i, j) + C_{12}(i, j)) (C_{24}(i, j) + C_{14}(i, j)), \end{aligned} \quad (47)$$

and  $D$  is the on-site double occupancy

$$D = \langle n_{i\uparrow}n_{i\downarrow} \rangle = \frac{n}{2} - C_{22}(i, i). \quad (48)$$

In the expression for  $\phi$ ,  $(i, j)$  denote nearest neighbour sites along the x-axis. We point out that Beenan and Edwards [7] used a simple factorization scheme for  $\theta$ . As these authors indicate [7], there is no unique way of performing this procedure. In our scheme, there are two distinct ways of decoupling the Green functions that lead to  $\theta$ . That is, we could have started with another Green function

$$H'(i, j, t, t') = \langle \langle c_\uparrow(i, t); c_\downarrow(i, t') c_\downarrow^\dagger(j, t') c_\uparrow^\dagger(j, t') \rangle \rangle. \quad (49)$$

Following the procedure outlined above, we arrive at the alternative expression for  $\theta$ :

$$\theta = \frac{2\zeta'}{\phi + 1}. \quad (50)$$

with

$$\begin{aligned} \zeta' &= \frac{2}{2 - n} (C_{11}(i, j) + C_{12}(i, j)) (C_{24}(i, j) + C_{14}(i, j)) \\ &\quad + \frac{2}{n} (C_{22}(i, j) + C_{12}(i, j)) (C_{13}(i, j) + C_{14}(i, j)). \end{aligned} \quad (51)$$

In the following section, we compare the values of  $\theta$  obtained by both methods.

Similarly it is possible to decouple the parameter  $p$  defined in Eq. (34). Because Eq. (34) contains only symmetric combinations of the fermionic operators, it

can be decoupled uniquely. From the procedure outlined above, we find that  $p$  is given by

$$p = \frac{n^2}{4} - \frac{\rho_1 + \phi\rho_2^2}{1 - \phi^2} - \frac{\rho_1 + \rho_2}{1 - \phi} - \frac{\rho_3}{1 + \phi} \quad (52)$$

where

$$\rho_1 = \frac{2}{2-n} (C_{11}(i,j) + C_{12}(i,j))^2 + \frac{2}{n} (C_{22} + C_{12})^2, \quad (53)$$

$$\rho_2 = \frac{2}{2-n} ((C_{13}(i,j) + C_{14}(i,j))^2 + \frac{2}{n} (C_{24} + C_{14})^2 \quad (54)$$

$$(55)$$

and

$$\rho_3 = \frac{4}{n(2-n)} (C_{11}(i,j) + C_{12}(i,j)) (C_{22} + C_{12}). \quad (56)$$

In the normal state,  $\rho_2 = 0$  as it contains only anomalous correlations and  $p$  reduces to the result derived by Roth [31]. The expressions for  $\theta$ ,  $p$  and the self-consistent equation for the correlation functions constitute the working equations of this method.

To summarize, the equations for  $\mathbf{M}$  and  $\mathbf{I}$  contain four parameters,  $\mu$ ,  $e$ ,  $p$  and  $\theta$  that must be determined self-consistently. From Eq. (33) and the definition of the Hubbard operators, the self-consistent equations for  $e$  and  $n$  are

$$e = C_{11}(i,j) - C_{22}(i,j) \quad (57)$$

$$n = 2(1 - C_{11}(i,i) - 2C_{12}(i,i) - C_{22}(i,i)). \quad (58)$$

In our computational procedure, we either used the two previous equations together with Eqs. (45) or (50). For the fourth self-consistent equation, we either used  $p$  or the equation that imposes the Pauli principle, Eq. (21).

#### IV. RESULTS

To set the stage for our results on the anomalous correlations, we discuss first the chemical potential. Shown in Fig. (1) are three different calculations of the chemical potential as a function of the filling: 1) solid line—present method, 2) dashed-dotted line—Beenan and Edwards [7], and 3) dashed line—Avella and co-workers [32]. Here,  $n = 1$  corresponds to half-filling. The method of Avella and co-workers [32] is identical to the method used here. However, as is evident, our results are significantly different. Particularly striking is the continuous increase of the chemical potential obtained by Avella and colleagues [32] as the filling is increased. This is in stark contrast our solution which levels off in the vicinity of half-filling. The difference between our treatments lies in that there are two solutions to the self-consistent equations. Avella and co-workers chose the solution that is higher in energy

in the filling range 0.7 – 1.0. While the lower energy solution is the physically-relevant solution, this solution in the absence of pairing has a distinct negative compressibility in the vicinity of half-filling. It is for this reason that Avella and co-workers [32] criticized, the method used by Roth as it also gives rise to a negative compressibility as seen from the dashed-dotted line of Beenan and Edwards [7]. Avella and co-workers [32] advocated that imposing the Pauli principle in the self-consistent solution to the equations of motion eliminates the negative compressibility.

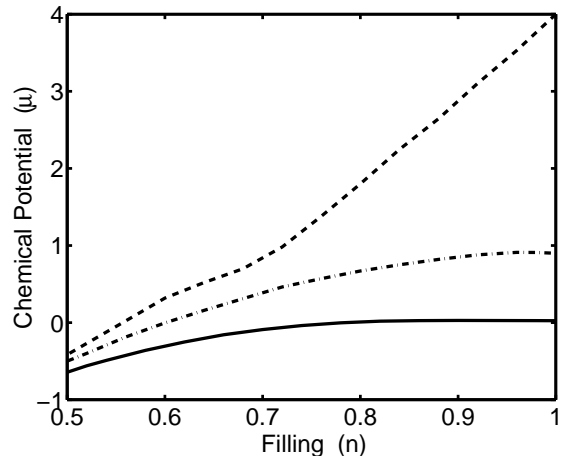


FIG. 1. The chemical potential (measured in units of the hopping  $t$ ) as a function of filling for  $U = 8t$  and  $T = 0$ .  $n=1$  corresponds to half filling. The dashed line corresponds to the work of Avella and colleagues [32] while the dashed -dotted line to the work of Beenan and Edwards [7]. Our work is the solid line and includes the effect of pairing.

Our work shows that even if the Pauli principle is maintained by means of Eq. (21), a second solution to the integral equations still exists along which the compressibility remains negative. To explore further the negative compressibility, we show in Fig. (2) the role of pairing on the compressibility. The dashed line corresponds to the chemical potential in the absence of pairing while along the solid line  $\theta \neq 0$ . As is evident, pairing alleviates the negative compressibility almost entirely giving rise to a flattening of the chemical potential in the vicinity of half-filling as seen from the solid curve in Fig. (2). In fact, a key trend common to the curves shown in Fig. (1) is that the compressibility is most positive when pairing vanishes. This result is particularly important because a negative compressibility occurs in numerous dilute electron systems, such as the 2D electron gas for  $r_s > 3$  [34]. Our results also corroborate the earlier observation of Tandon, Wang, and Kotliar [35] that the compressibility becomes negative in the  $U \rightarrow \infty$  Hubbard model. For short-range Coulomb interactions, a negative compressibility signifies that the ground state of an electronic system is unstable relative to a uniform charge distribution.

Hence, a negative compressibility is typically associated with phase separation or stripe formation [36]. Our work explicitly shows that pairing alleviates this instability at least in the case of short-range Coulomb interactions. We have proposed that even in the case of long-range Coulomb interactions, pairing still obtains and alleviates the negative compressibility as well [37].

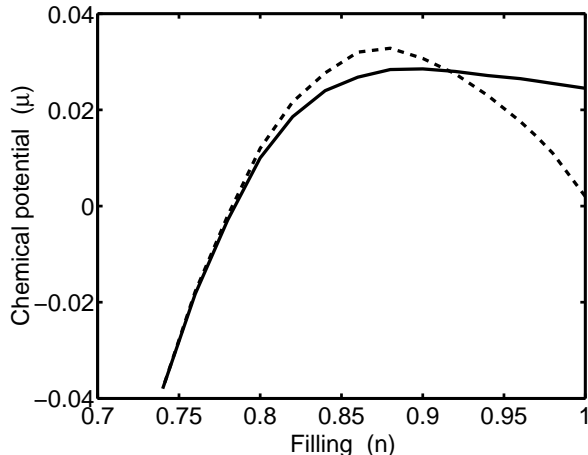


FIG. 2. The chemical potential as a function of filling for  $U = 8t$  and  $T = 0$  in the absence of pairing (dashed line) and in the presence of pairing (solid line). The chemical potential is in units of  $t$ . The solid line clearly illustrates that pairing alleviates the negative compressibility.

We now discuss explicitly the anomalous correlation functions. Shown in Fig. (3) are four different calculations of the correlation function involving pairing of composite excitations. The two solid lines in Fig. (3) were obtained from Eq. (50). On the upper curve, the Pauli principle was imposed whereas along the lower curve, the decoupling scheme was used to calculate the parameter  $p$  defined in Eq. (34). Hence, the lower curve corresponds to the method of Beenan and Edwards [7]. On the dashed curves, Eq. (45) was used to compute  $\theta$ . Once again, along the upper dashed curve, the Pauli principle was used whereas along the lower curve, the decoupling scheme (for  $p$ ) was used. Our results indicate that the anomalous correlations are largest and most stable when the Pauli principle is imposed by using the integral equation, Eq. (21). When the decoupling scheme is used to obtain  $p$ , the two distinct decouplings for  $\theta$  yield vastly different results. This will result in huge fluctuations in  $T_c$  as the work of Beenan and Edwards [7] illustrates. What our work establishes is that if the Pauli principle is imposed in the self-consistent procedure outlined here, consistent pairing solutions exist regardless of the decoupling scheme used to calculate  $\theta$ . Note also that the two lower curves are peaked around a doping level of 20%. Beenan and Edwards [7] associated great significance to this doping level as it corresponds to the filling at which the Fermi surface resembles the Fermi surface at half-

filling for the non-interacting system. This appears to be an accident of their approximations as our more accurate method shows that the peak in the order parameter occurs at a doping level of 10%.

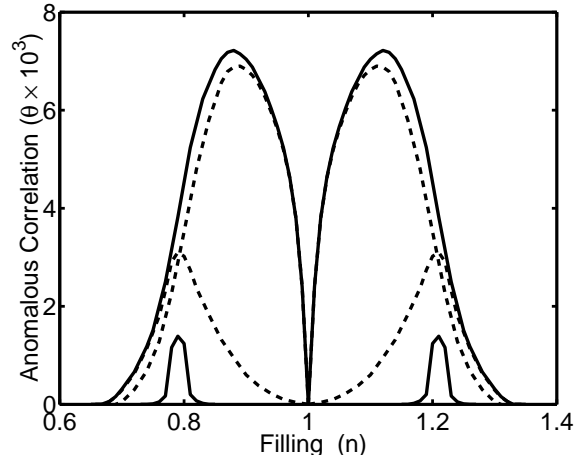


FIG. 3. Anomalous pairing correlation as a function of filling for  $U = 8t$  and  $T = 0$ . The two solid lines were obtained from Eq. (50). On the upper curve, the Pauli principle was imposed whereas along the lower curve the decoupling scheme was used to calculate Eq. (34). On the dashed curves, Eq. (45) was used to compute  $\theta$ . Once again, along the upper dashed curve, the Pauli principle was used whereas along the lower curve the decoupling scheme for  $p$  was used. Our results indicate that the anomalous correlations are largest and most stable when the Pauli principle is imposed.

The remaining figures constitute the primary results of this method. Shown in Fig. (4) is a calculation of  $\theta$  in which the average of Eq. 45) and (50) as a function of filling was used. Our results show clearly that  $d_{x^2-y^2}$  pairing exists and such pairing is diminished as  $U$  increases. As our method is valid only in the large  $U$  limit, we cannot establish the lower value of  $U/t$  for which  $\theta$  is non-zero. Also of significance is the maximum in  $\theta$  at roughly 10% doping for the range of on-site repulsions studied. In addition, the peak in  $\theta$  moves to higher dopings as  $U$  increases. We emphasize that the pair-formation found here does not include the effect of phase fluctuations. Hence, the actual doping regime over which true superconductivity with long-range order occurs might be significantly smaller than that obtained here. For example, if long-range order obtains at all, the optimum doping will appear shifted to higher doping values relative to the maxima of the curves shown here. Preliminary results by Manske, Dahm and Bennemann [38] using phenomenological spin-fluctuation approximations offer some support of this conclusion. Also of note is the fact that our treatment preserves the particle-hole symmetry of  $\theta$ . The temperature dependence of the order parameter is shown in Fig. (5). As is evident, the shape of  $\theta$  is characteristic of any order parameter that vanishes at a transition temperature. For  $U = 8t$ , we find that the



onset temperature,  $T^* = .021t$ . In the cuprates  $t = .5eV$ . Hence, we obtain an onset temperature of  $T^* = 100K$  for pair formation. Phase coherence occurs at a lower temperature,  $T_c$ . As a consequence, the  $T^*$  calculated here should serve as a realistic estimate of the pseudogap temperature [39]. At optimum doping,  $T^*$  should correspond to  $T_c$ . Experimentally, optimal doping corresponds to roughly 20%. At this doping level and for  $U = 8t$ , we obtain that  $T_c = 65K$  leading to a ratio of  $T^*/T_c = 1.5$ . For  $YBa_2Cu_3O_{6.95}$ ,  $T_c = 92K$  while  $T^* = 110K$  [40]. Typically in the cuprates,  $1.2 < T^*/T_c < 2$  in the underdoped regime [39]. While our calculated values for  $T^*$  and  $T_c$  are not rigorous estimates, it is encouraging that they are not far off from the experimental values.

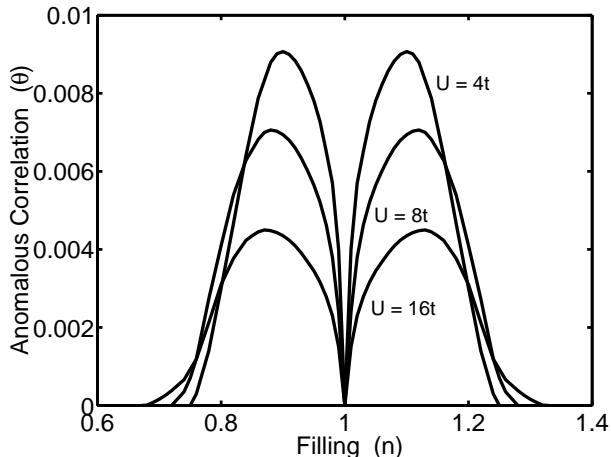


FIG. 4. Anomalous pairing correlation function as a function of filling for various values of  $U$  for  $T = 0$ . We obtained  $\theta$  taking the average of Eqs. (45) and (50).

## V. FINAL REMARKS

We have presented here an analysis ideally suited for the strong-coupling limit of the Hubbard model. Two key results are established. First, pairing in the Hubbard model occurs in the  $d_{x^2-y^2}$  channel. Second, composite excitations rather than electron-like excitations pair together. They live on a cluster of nearest-neighbour sites and are formed out of a hole and a singly-occupied site. Ultimately, such excitations could explain the absence of a well-defined electron-like peak in the ARPES experiments [14] if the self-energy correction in Eq. (17) arising from the dynamical processes significantly broadens the energy levels near the Fermi energy. Sasaki, Matsumoto and Tachiki [41] have evaluated such dynamical corrections in the context of the p-d model for the cuprates and found that the composite operator spectrum remains intact (thereby justifying the initial choice of the composite operator basis); however, broadening of all levels including those at the Fermi surface was observed. Matsumoto and Mancini [42] have also performed similar calculations

for the Hubbard model [42] and observed a broadening of the levels at the Fermi surface.

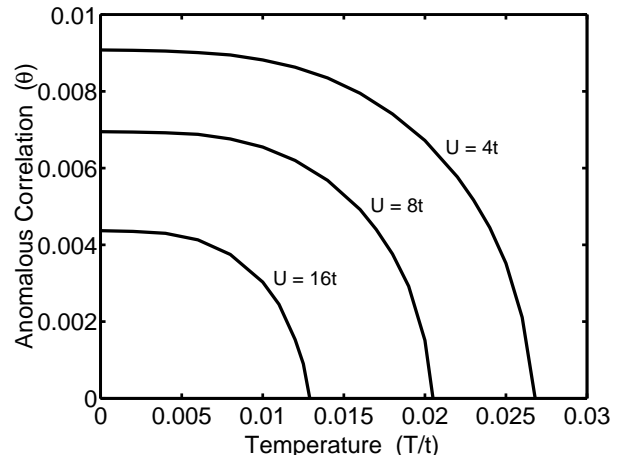


FIG. 5. Temperature dependence of the anomalous correlation function at  $n = .9$ , the optimal doping as found in Fig. (4). All quantities are measured in units of  $t$ . The overall shape of  $\theta(T)$  is consistent with the interpretation that  $\theta$  is a pairing gap.

Longer-range Coulomb interactions, necessitate the retention of higher-order composite excitations. The simplest of such excitations will involve three sites. Computing the equations of motion for the three-site composite excitations leads 4-site excitations. At each iteration of this procedure, the range of the composite excitations grows. We have verified that nearest-neighbour repulsive Coulomb interactions drastically diminish the anomalous pairing in  $\theta$ . Trivially, attractive nearest-neighbour Coulomb interactions enhance pairing. However, to completely settle the issue of pairing when repulsive next-nearest neighbour interactions are included, we must also retain the anomalous correlation functions that are generated in the presence of the longer-range interaction. Our work here suggests that such correlation functions should be computed to determine if composite particle pairing survives in the extended Hubbard model.

Nonetheless, within the on-site repulsive model, the correlation function ( $\theta$ ) calculated here should be sufficient to describe the pairing process. Because  $\theta$  involves a product of the form  $\eta_{ij\uparrow}\eta_{ij\downarrow}$ , the pairing mechanism is entirely local. From the form of  $\eta_{ij}$ , it is tempting to conclude that pairing requires a doubly-occupied site to neighbour a singly-occupied site. In such a configuration, double occupancy can be shared between the two sites. However, this is just one of the many types of local configurations that gives rise to a non-zero value of  $\theta$ . If long-range phase coherence obtains, one can think of the condensate as a coherent superposition of all such resonating structures. This suggests that the pair-pair correlation function for the cexons should be calculated to verify one way or another if phase coherence obtains.

\*Current Address: Theory Division, Los Alamos National Laboratory.

### ACKNOWLEDGMENTS

We thank P. Wolynes, A. Yazdani, and T. Leggett for helpful conversations and the NSF grant No. DMR98-96134.

- 
- [1] J. R. Hirsch, Phys. Rev. Lett. **54**, 1317 (1985); D. J. Scalapino, Phys. Reports, **250**, 329 (1995); For a review see E. Dagotto, Rev. Mod. Phys. **67**, 63 (1994).
  - [2] S. Zhang, J. Carlson, and J. E. Gubernatis, Phys. Rev. Lett. **78**, 4486 (1997).
  - [3] S. Mazumdar, R. T. Clay, and D. K. Campbell/condmat-9910164.
  - [4] T. Husslein, et. al. unpublished.
  - [5] K. Kuroki and T. Aoki, Phys. Rev. B **57** R14287, (1997).
  - [6] N. E. Bickers, D. J. Scalapino and S. R. White, Phys. Rev. Lett. **62**, 961 (1989).
  - [7] J. Beenen and D. M. Edwards, Phys. Rev. B **52**, 13636 (1995).
  - [8] F. Manicni, S. Marra and H. Matsumoto, Physica C **252**, 361 (1995).
  - [9] P. W. Anderson, Science **235**, 1196 (1987).
  - [10] J. Hubbard, Proc. Roy. Soc. A **276**, 238 (1963).
  - [11] A. Dorneich, M. G. Zacher, C. Gröber and R. Eder, condmat/9909352.
  - [12] K. Kuroki, H. Aoki, T. Hotta, and Y. Takada, Phys. Rev. B **55**, 2764 (1997).
  - [13] E. Dagotto and J. R. Schrieffer, Phys. Rev. B **43**, 8706 (1991).
  - [14] Z. X. Shen and D. S. Dessau, Phys. Rep. bf 253, 1 (1995); For a review see M. Randeria and J. -C. Campuzano, *Varenna Lectures* condmat/9709107.
  - [15] T. Senthil and M. P. A. Fisher, condmat/9912380.
  - [16] J. M. Luttinger, Phys. Rev **119**, 1153 (1960).
  - [17] R. B. Laughlin, Phys. Rev. Lett. **50**, 873 (1983).
  - [18] V. J. Goldman and B. Su, Science bf 267, 1010 (1995); de Picciotto, et. al. Nature **389**, 162 (1997); L. Saminadayar and D. C. Glatthli, Phys. Rev. Lett. **79**, 2526 (1997); A. M. Chang, L. N. Pfeiffer, and K. West, Phys. Rev. Lett. **77**, 2538 (1996).
  - [19] G. Baskaran, Z. Zou, and P. W. Anderson, Solid State Comm. **63**, 973 (1987).
  - [20] G. Baskaran and P. W. Anderson, Phys. Rev. B, **37**, 580 (1988).
  - [21] G. Kotliar and L. Jialin, Phys. Rev. B **38**, 5142 (1988).
  - [22] L. B. Ioffe and A. I. Larkin, Phys. Rev. B **39**, 8988 (1989).
  - [23] P. A. Lee and N. Nagaosa, Phys. Rev. B **46**, 5621 (1992).
  - [24] A. M. Tikofsky and R. B. Laughlin, Phys. Rev. B **50**, 10165 (1994).
  - [25] B. L. Altshuler, L. B. Ioffe, and A. J. Millis, Phys. Rev. B **53**, 415 (1996).
  - [26] X. G. Wen and P. A. Lee, Phys. Rev. Lett. **76**, 503 (1996).
  - [27] D. H. Kim and P. A. Lee, Ann. Phys. **272**, 130 (1999).
  - [28] C. Nayak, cond-mat/9912270.
  - [29] K. Park, V. Melik-Alaverdian, N. H. Bonesteel, and J. K. Jain, Phys. Rev. B **58**, R10167 (1998).
  - [30] J. Lindeberg and Y. Öhrn, Chem. Phys. Lett. **1**, 295 (1967).
  - [31] L. M. Roth, Phys. Rev. **184**, 451 (1969).
  - [32] F. Mancini, Phys. Lett. A **249**, 231 (1998); for a review see S. Avella, F. Mancini, D. Villani, L. Siurakshina, V. Yu. Yushmankhai, Int. J. Mod. Phys. B **12**, 81 (1998).
  - [33] S. Ishihara, et. al. Phys. Rev. B **49**, 1350 (1994).
  - [34] S. Moroni, D. Ceperley, and G. Senatore, *Proc. Rochester Symp. Coupled Plasmas*, eds. H. van Horn and S. Ichimaru (Univ. Rochester Press, 1993) p. 445.
  - [35] A. Tandon, Z. Wang, and G. Kotliar, Phys. Rev. Lett. **83** 2046 (1993).
  - [36] J. Zaanen and O. Gunnarsson, Phys. Rev. B **40**, 7391 (1989); see also S. A. Kivelson and V. J. Emery, Synth. Met. **80**, 151 (1996).
  - [37] P. Phillips, et. al. Nature (London) **253**, 395 (1998).
  - [38] D. Manske, T. Dahm, and K. H. Bennemann, condmat/9912062.
  - [39] For a review see T. Timusk and B. Statt, Rep. Prog. Phys. **62**, 61 (1999).
  - [40] J. A. Martindale and P. C. Hammel, Phil. Mag. B **74**, 573 (1996).
  - [41] M. Sasaki, H. Matsumoto, and M. Tachiki, Phys. Rev. B **46**, 3022 (1992).
  - [42] H. Matsumoto and F. Mancini, Phys. Rev. B **55**, 2095 (1997).